The Mechanical Energy Input to the Ocean Induced by Tropical Cyclones

LING LING LIU AND WEI WANG

Physical Oceanography Laboratory, Ocean University of China, Qingdao, Shandong, China

RUI XIN HUANG

Department of Physical Oceanography, Woods Hole Oceanographic Institution, Woods Hole, Massachusetts

ABSTRACT

Wind stress and tidal dissipation are the most important sources of mechanical energy for maintaining the oceanic general circulation. The contribution of mechanical energy due to tropical cyclones can be a vitally important factor in regulating the oceanic general circulation and its variability. However, previous estimates of wind stress energy input were based on low-resolution wind stress data in which strong nonlinear events, such as tropical cyclones, were smoothed out.

Using a hurricane–ocean coupled model constructed from an axisymmetric hurricane model and a three-layer ocean model, the rate of energy input to the world's oceans induced by tropical cyclones over the period from 1984 to 2003 was estimated. The energy input is estimated as follows: 1.62 TW to the surface waves and 0.10 TW to the surface currents (including 0.03 TW to the near-inertial motions). The rate of gravitational potential energy increase due to tropical cyclones is 0.05 TW. Both the energy input from tropical cyclones and the increase of gravitational potential energy of the ocean show strong interannual and decadal variability with an increasing rate of 16% over the past 20 years. The annual mean diapycnal upwelling induced by tropical cyclones over the past 20 years is estimated as 39 Sv (Sv $\equiv 10^6$ m^3 s^{-1}). Owing to tropical cyclones, diapycnal mixing in the upper ocean (below the mixed layer) is greatly enhanced. Within the regimes of strong activity of tropical cyclones, the increase of diapycnal diffusivity is on the order of $(1 - 6) \times 10^{-4}$ m^2 s^{-1}. The tropical cyclone–related energy input and diapycnal mixing may play an important role in climate variability, ecology, fishery, and environments.

1. Introduction

Although oceans receive a huge amount of thermal energy, such energy cannot be efficiently converted into mechanical energy because the ocean is heated and cooled from the same geopotential level, the upper surface. Therefore, in order to maintain the quasi-steady oceanic circulation external sources of mechanical energy are required to balance the loss of mechanical energy due to friction and dissipation. It is only within the past 10 years that the oceanography community has come to realize the vital importance of external sources of mechanical energy in maintaining and regulating the oceanic general circulation. Wind stress and tidal dissipation are the primary sources of mechanical energy. The contribution due to tidal dissipation in the open ocean is estimated as 0.7–0.9 TW (Munk and Wunsch 1998). However, wind energy input may play an even more important role, especially in the upper kilometer of the open ocean. Wind stress energy input to the surface geostrophic currents is estimated as 0.88 TW (Wunsch 1998; Huang et al. 2006). Wind stress energy input to the surface waves is estimated as 60 TW (Wang and Huang 2004a). Wind stress energy input to the Ekman layer is estimated as 0.5–0.7 TW over the near-inertial frequency (Alford 2003; Watanabe and Hibiya 2002), and the energy input over the subinertial range is about 2.4 TW (Wang and Huang 2004b).

However, some important sources of mechanical energy in the world's oceans remain unaccountable. Strong nonlinear events in the weather system, such as tropical cyclones, belong to this category. Tropical cyclone activity is a vitally important component of the atmospheric circulation system at low- and midlatitudes. In the commonly used low spatial resolution wind stress data, such as the National Centers for Environmental Prediction–National Center for Atmo-

Corresponding author address: Wei Wang, Physical Oceanography Laboratory, Ocean University of China, Qingdao 266003, Shandong, China.
E-mail: wei@ouc.edu.cn

spheric Research (NCEP–NCAR) reanalysis, these strong nonlinear events are smoothed out. As a result, their contributions to the global mechanical energy input are excluded.

Emanuel (2001) argued that subtropical cyclones are one of the strongest time-varying components in the atmospheric circulation. The activity of tropical cyclones has been enhanced during the past decades, apparently due to global warming. Accordingly, great changes in the energy input to the ocean induced by tropical cyclones are expected.

Recently, Huang et al. (2007) have shown that deepening of the mixed layer at low latitudes can enhance the meridional pressure difference and thus the overturning circulation and poleward heat flux. The strong activity of subtropical cyclones can deepen the mixed layer at low latitudes. Owing to the strong wind associated with the subtropical cyclones, mixing in the ocean is greatly enhanced (Sriver and Huber 2007). These authors presented the annualized vertical diffusivity attributable to cyclone mixing, which is ranged by a factor of 30 compared to the microstructure-based measurements. The strong ocean mixing induced by tropical cyclones may play vitally important roles in the oceanic general circulation and the climate.

The main goal of this study is to estimate the energy input to the world's oceans induced by tropical cyclones, including the energy input to surface waves, surface currents, and in particular the near-inertial motions in the mixed layer. The estimates of the energy input from tropical cyclones to the ocean are based on a hurricane–ocean coupled model. Meanwhile, a simple slab model is used to estimate the increase of the gravitational potential energy (GPE) in the oceanic surface mixed layer. In addition, the annual mean upwelling rate and vertical diffusivity induced by tropical cyclones in the world's oceans are estimated.

The formulation of the hurricane–ocean coupled model and the techniques for estimating the energy input to the ocean by tropical cyclones are discussed in section 2. The oceanic response to a moving tropical cyclone is described in detail in section 3. The temporal evolution of a typical hurricane and the distribution of the mechanical energy sources are discussed in section 4. The variability of the annual-mean energy input from the tropical cyclones over the world's oceans from 1984 to 2003 is discussed in section 5. Finally, we conclude in section 6.

2. Model formulation

The hurricane–ocean coupled model used in this study consists of two independently developed and tested models, that is, the axisymmetric hurricane model of Emanuel (1989) and the four-layer ocean model of Cooper and Thompson (1989). The formulation of both models has been described in detail in the cited references; the principal physical processes, the balances, and the coupling procedure were described by Schade and Emanuel (1999). Price (1981) suggested that much of the entrainment arises from turbulence associated with velocity shears at the base of the mixed layer, rather than through the effect of surface-generated turbulence. Therefore, in this study, Price's (1981) formulation based on the Richardson number is used to parameterize the entrainment.

The tracks of tropical cyclones from observations, as composed on K. A. Emanuel's Web site (ftp://texmex.mit.edu/pub/emanuel/HURR/tracks/), will be used in our calculation. The following list includes the differences between our model and that of Schade and Emanuel (1999). In particular, changes along the tracks were taken into account.

1) Variation of Coriolis parameter f along the track and the variation of the translation speed with time estimated from "best track" data were taken into consideration in our calculations.
2) The initial state of the model ocean is inhomogeneous in the along-track direction. The temperature field is based on the Levitus98 monthly temperature field, and the initial mixed layer depth is calculated from the monthly mean climatology, using the criterion that temperature at the base of the mixed layer is 0.1°C lower than that at the sea surface. In the model, the initial temperature of the mixed layer is set to the surface temperature from the Levitus98 monthly temperature field; however, between the mixed layer and the thermocline there is an infinite thin layer with a temperature jump of 0.1°C.
3) In some previous models the temperature of the water entrained into the mixed layer was set to the temperature at the top of the thermocline. The corresponding temperature jump at the base of mixed layer was usually chosen as 1°C. In our model, we first determine the thickness of the entrained water from the thermocline below; then the mean temperature of this water column is used as the temperature of the entrained water.

Wind stress was calculated using the bulk formula

$$\tau = \rho_a C_D |u|u, \quad C_D = 0.001 \times (0.73 + 0.069u), \quad (1)$$

where τ is the wind stress vector, $\rho_a = 1.26$ kg m^{-3} is the density of air, C_D is the drag coefficient in a composite form (Garrett 1977), u is the speed of the geostrophic
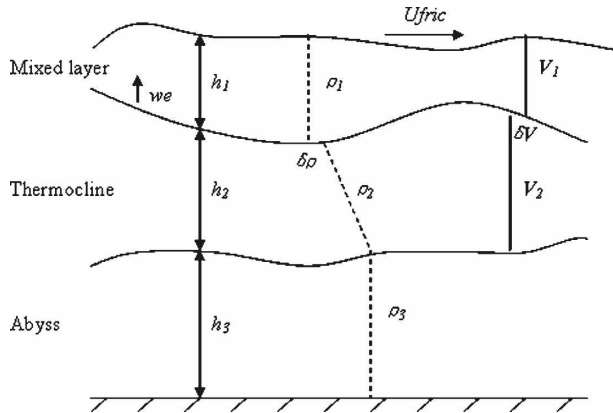
FIG. 1. Sketch of the model ocean, with a mixed layer with uniform density on the top, a thermocline layer in the middle, and a thick and stagnant abyssal layer on the bottom. Note that there is a density jump across the base of the mixed layer.

wind 10 m above the sea surface, and u is the wind vector.

The temporal resolution of the ocean model is 5 min and the ocean model has a horizontal dimension of 1500 km × 5000 km with a horizontal resolution of 5 km × 5 km. There are three layers: a well-mixed layer on the top, a strongly stratified layer in the middle, and a deep and stagnant abyssal layer on the bottom (Fig. 1). Temperature in the thermocline is assumed to be a linear function of depth. Momentum is turbulently exchanged through the air–sea interface. In the ocean interior, vertical exchange of mass and heat is allowed only between the mixed layer and the thermocline.

The model is formulated in a coordinate system moving with the center of the tropical cyclone as follows: The center of the tropical cyclone is initially located at the center of the model domain and moves westward in this coordinate with a speed calculated using the observed track data. Before the center of the tropical cyclone reaches the next grid point west of the current origin of the coordinates, all variables in the ocean model are calculated in terms of Eulerian coordinates fixed in space. However, as the center of the tropical cyclone moves beyond the next grid point, all variables in the ocean model will be shifted eastward for one grid point. All variables along the western boundary will be set to the initial values calculated from the monthly mean climatology by interpolation; in particular, the velocity will be set to zero. Since the typical migration speed of the tropical cyclone is about 5 m s^{-1}, the typical time for the grid shifting in the model is about 15 min; that is, the grid is shifted roughly every three time steps in the ocean model. Of course, the real situation is more complicated, and the shifting time of the grid varies from time to time and case to case.

The atmospheric component of the coupled hurricane model is axisymmetric in gradient wind and hydrostatic balance and consists of three layers: a boundary layer and two tropospheric layers. In the radial direction, the model uses angular momentum coordinates, that is, $fR^2 = 2rV + fr^2$, where R is the potential radius, V is the velocity of air flowing around the storm, r is the physical radius, and f is the Coriolis parameter. For results presented in the following discussion, there are 46 radial nodes that span 2000 km and the time step is 0.5 min.

Aside from the effect of radial diffusion, angular momentum is strictly conserved in the interior of the atmosphere model. Similar to the balance of momentum, heat is transferred turbulently between atmosphere and ocean, and this transfer is parameterized in terms of the bulk aerodynamic drag law. However, there are two nonconservative processes included in the model in the atmosphere interior. First, the release of latent heat due to phase changes of water is treated implicitly by using moist entropy as a combined temperature and humidity variable. Second, radiative cooling is crudely parameterized as a Newtonian relaxation back to the initial convectively neutral sounding (Schade and Emanuel 1999).

In summary, the ocean model is forced by the surface wind field constructed from the axisymmetric flow in the hurricane model with the translation velocity of the hurricane. In turn, the hurricane model is forced by an axisymmetric SST field constructed through azimuthal averaging of the SST field around the center of the hurricane obtained from the ocean model. The respective forcing fields are updated each time step.

a. Energy input to the ocean

1) SURFACE WAVES

One of the major forms of energy transfer from wind to the ocean is through surface waves. The total amount of mechanical energy input to surface waves in the world's oceans with low spatial resolution wind stress data (NCEP–NCAR) was estimated as 60 TW (Wang and Huang 2004a). By comparing three different approaches, Wang and Huang (2004a) concluded that the energy input to surface waves induced by wind stress can be estimated by the following simple formula:

$$q_{\text{wave}} = \int\!\!\int_A 3.5\rho_a u_{*a}^3 \, dx \, dy, \qquad (2)$$

where $u_{*a} = \sqrt{\tau/\rho_a}$, ρ_a is density of air, τ is the wind stress, and A is the horizontal area affected by the tropical cyclone. In this study, this formula will be used to

estimate mechanical energy input to surface waves induced by tropical cyclones.

2) SURFACE CURRENTS

The wind energy input to surface currents was calculated as

$$q_{\text{current}} = \iint_A \boldsymbol{\tau} \cdot \mathbf{u}_s \, dx \, dy. \tag{3}$$

The wind stress and velocity were obtained from the coupled model. Here, the surface velocity $\mathbf{u}_s$ denotes the total velocity in the mixed layer, including both the geostrophic and ageostrophic components.

3) NEAR-INERTIAL FREQUENCY OSCILLATIONS

Energy input to surface current covers a wide spectrum and, in particular, it includes energy input to the near-inertial motions, which are the most likely contributors to the subsurface turbulence, internal waves, and the subsurface diapycnal mixing. The energy source associated with the wind generated near inertial oscillations is, thus, of great interest to our understanding of the energetics of the oceanic circulation and the deepening of the mixed layer.

Tropical cyclones are excellent generators of near-inertial motions because of their large wind stress that change on the inertial time scale. The generation of inertial motions by tropical cyclones has been discussed in previous studies (e.g., Price 1981, 1983). Near-inertial oscillations constitute a vitally important part of the dynamic response of the upper ocean to wind forcing.

Energy input to near-inertial motions in the world's oceans, based on smoothed wind stress data, was estimated as 0.5–0.7 TW (Watanabe and Hibiya 2002; Alford 2003). These studies used the same formulation for estimating the kinetic energy (KE) flux from the wind to inertial motions introduced by D'Asaro (1985), including a simple damped slab model of Pollard and Millard (1970).

Recently, Plueddemann and Farrar (2006) introduced a new formulation for estimating the kinetic energy flux induced by strong forcing events to inertial motions using the Price–Weller–Pinkel (PWP) mixed layer model (Price et al. 1986). In this study we will use a similar approach to study the energy input to near-inertial oscillations from wind stress associated with tropical cyclones.

With the additional assumption that horizontal property gradients can be neglected the momentum equations are

$$\frac{\partial u}{\partial t} - fv = -\frac{1}{\rho_0} \frac{\partial p}{\partial x} + \frac{\tau_W^x - \tau_R^x}{\rho_0 h_1},$$

$$\frac{\partial v}{\partial t} + fu = -\frac{1}{\rho_0} \frac{\partial p}{\partial y} + \frac{\tau_W^y - \tau_R^y}{\rho_0 h_1}, \tag{4}$$

where (u, v) are the horizontal velocity components in the mixed layer, f is the Coriolis parameter, (τ_W^x, τ_W^y) are the surface wind stress components, p is the pressure, ρ_0 is the reference density, (τ_R^x, τ_R^y) represent the momentum flux associated with the entrainment process, and h_1 is the mixed layer thickness.

Paralleling D'Asaro (1985) and adopting the complex notation, we decompose the complex velocity $Z = u + iv$ into three components:

$$Z = Z_I + Z_g + Z_E, \tag{5}$$

where $Z_g = -\boldsymbol{\nabla}p/if$ is the geostrophic currents, Z_I is damped inertial oscillation, and

$$Z_E = (T_W - T_R)/ifh_1 \tag{6}$$

is the time-varying Ekman current, where $T_W = (\tau_W^x + i\tau_W^y)/\rho_0$ and $T_R = (\tau_R^x + i\tau_R^y)/\rho_0$. Thus, (4) is reduced to

$$\frac{\partial Z_I}{\partial t} + ifZ_I = -\frac{1}{if} \frac{\partial}{\partial t} \left(\frac{T_W}{h_1} - \frac{T_R}{h_1} - \boldsymbol{\nabla}p \right). \tag{7}$$

Multiplying (7) by $\rho_0 h_1 Z_I^*$, where Z_I^* is the complex conjugate of Z_I, gives rise to the kinetic energy balance equation for the mixed layer, and the corresponding energy flux within the affected area due to wind forcing (Plueddemann and Farrar 2006),

$$q_{\text{ni}} = \iint_A -\rho_0 h_1 \, \text{Re} \left[\frac{Z_I^*}{if} \frac{\partial}{\partial t} \left(\frac{T_W}{h_1} \right) \right] dx \, dy. \tag{8}$$

Near-inertial motions constitute an important part of the kinetic energy in the mixed layer. For example, there is a clearly defined power spectral peak between $0.9f$ and $1.26f$ in the power spectral of mixed layer currents at a given point (Fig. 2). The actual calculations were carried out, using near-inertial velocity extracted from the mixed layer velocity. In Eq. (8) the mixed layer thickness and wind stress were from the model output and the Coriolis parameter f was calculated from the "best track" data.

b. The increase of the gravitational potential energy

Tropical cyclone–induced cooling in the upper ocean is a striking phenomenon that is one of the important consequences of the interaction between tropical cyclones and the ocean (Emanuel 1988). Since the hurricane-induced surface cooling can be observed from both satellites and in situ instruments, it has been docu-
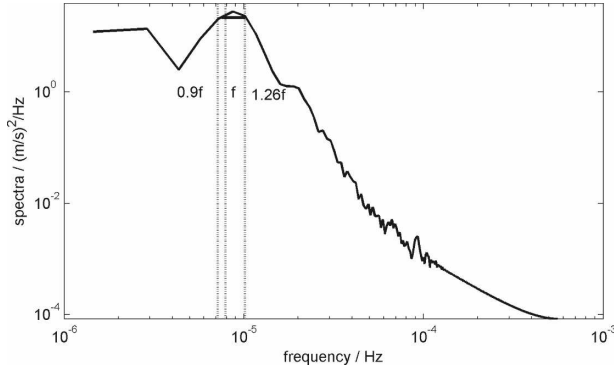
FIG. 2. The power spectrum of kinetic energy of mixed layer currents at a fixed station. The local inertial frequency is denoted by the vertical line labeled by f.
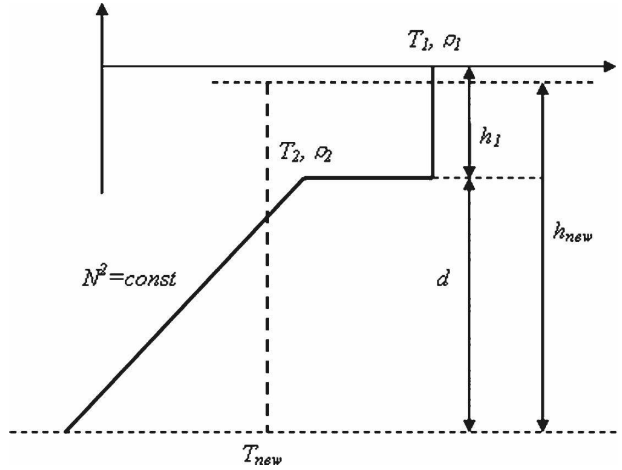

FIG. 3. Sketch of the mixed layer before and after the tropical cyclone. In the thermocline layer, $N^2 = -(g/\rho_0)(\partial\rho/\partial z) = g\alpha(\partial T/\partial z) = \text{const}$.

mented in many studies. Emanuel (2001) postulated that much of the observed lateral heat fluxes in the ocean is induced by tropical cyclones. Within the vicinity of a tropical cyclone, strong winds blowing across the sea surface drive strong ocean currents in the mixed layer. The vertical shear of the horizontal current at the base of the mixed layer induces strong turbulence, driving mixing of warm/cold water across the mixed layer base (Emanuel 2005). As a result, sea surface temperature is cooled down. Most importantly, the warming of water below the mixed layer raises the center of mass, and the GPE of the water column is increased.

Price (1981) modeled the response of the upper ocean to tropical cyclones and demonstrated that about 85% of the observed surface cooling results from entrainment, with the remainder owing to surface heat fluxes. Therefore, during the stirring of a tropical cyclone the air–sea heat exchange is negligible in the calculation of surface cooling. Furthermore, the mass loss due to evaporation is only a tiny part of the total mass involved in the mixing processes. Thus, as an approxi-

mation, we can assume the conservation of heat and mass during the wind stirring.

The structure of the mixed layer before and after the passing of a tropical cyclone at a fixed station is schematically shown in Fig. 3: h_1 is the initial thickness of mixed layer, T_1 is SST, and T_2 is the temperature at the top of the thermocline; h_{new} and T_{new} are the thickness and temperature of the mixed layer after stirring, d is the thickness of the thermocline that is stirred by the tropical cyclone, and N is the Brunt–Väisälä frequency.

In the model, density is assumed to be a linear function of temperature

$$\rho = \rho_0[1 - \alpha(T - T_0)], \qquad (9)$$

where $\rho_0 = 1023.5$ kg m^{-3} is the reference density, $T_0 = 27°$C the reference temperature, and $\alpha = 3.3 \times 10^{-4}$ °C^{-1} the mean thermal expansion coefficient. The mass, heat content, and GPE (per unit area) of the initial state are

$$M_1 = \int_0^d \rho\, dz + \int_d^{d+h1} \rho\, dz = \int_0^d \left[\rho_2 - \frac{\rho_0 N^2}{g}(z-d)\right] dz + \int_d^{d+h_1} \rho_1\, dz = \frac{1}{2}\frac{\rho_0 N^2}{g\alpha}d^2 + \rho_2 d + \rho_1 h_1, \qquad (10)$$

$$J_1 = \int_0^d \rho C_p T\, dz + \int_d^{d+h_1} \rho C_p T\, dz = \int_0^d C_p \cdot \left[\rho_2 - \frac{\rho_0 N^2}{g}(z-d)\right] \cdot \left[T_2 + \frac{N^2}{g\alpha}(z-d)\right] dz + \int_d^{d+h_1} \rho_1 C_p T_1\, dz$$

$$= C_p\left(-\frac{1}{3}\frac{\rho_0 N^4}{g^2\alpha}d^3 + \frac{1}{2}\frac{\rho_0 N^2}{g}T_2 d^2 - \frac{1}{2}\frac{\rho_2 N^2}{g\alpha}d^2 + \rho_2 T_2 d + \rho_1 T_1 h_1\right), \qquad (11)$$

$$\chi_1 = \int_0^d \rho g z\, dz + \int_d^{d+h_1} \rho g z\, dz = \int_0^d \left[\rho_2 - \frac{\rho_0 N^2}{g}(z-d)\right] g z\, dz + \int_d^{d+h_1} \rho_1 g z\, dz$$

$$= \left(\frac{1}{6}\frac{\rho_0 N^2}{g}d^3 + \frac{1}{2}\rho_2 d^2 + \rho_1 h_1 d + \frac{1}{2}\rho_1 h_1^2\right)g, \qquad (12)$$
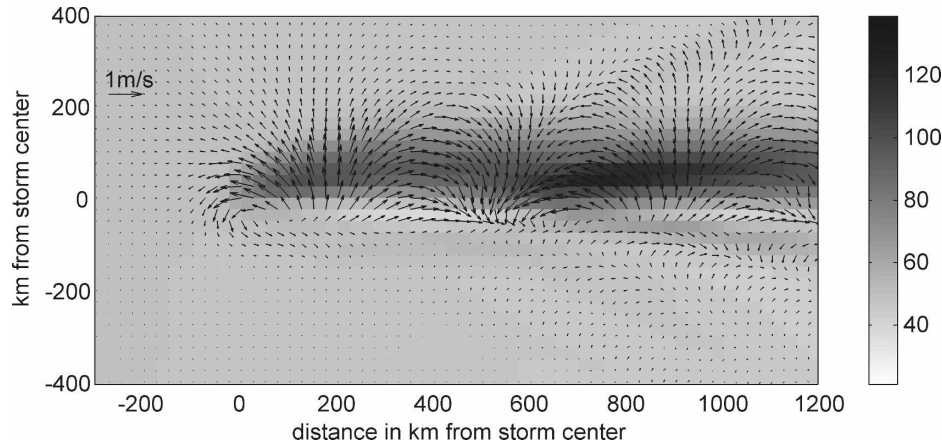
FIG. 4. The horizontal distribution of surface currents and the mixed layer depth forced by a hurricane moving westward. The direction of ocean currents is depicted by black arrows, whose length is proportional to the speed. The colors indicate the depth (m) of the ocean mixed layer.

where the base of the mixed layer after mixing is chosen as the reference level of GPE. The corresponding mass, heat content, and GPE (per unit area) after stirring of tropical cyclones are

$$M_2 = \int_0^{h_{new}} \rho \, dz = \rho_{new} h_{new}, \tag{13}$$

$$J_2 = \int_0^{h_{new}} \rho C_p T \, dz = \int_0^{h_{new}} \rho_{new} C_p T_{new} \, dz$$

$$= C_p \rho_{new} T_{new} h_{new}, \tag{14}$$

$$\chi_2 = \int_0^{h_{new}} \rho g z \, dz = \int_0^{h_{new}} \rho_{new} g z \, dz = \frac{1}{2} \rho_{new} g h_{new}^2. \tag{15}$$

The increment of GPE per unit area is increased

$$\Delta\chi = \chi_2 - \chi_1 = \frac{1}{2} \rho_{new} g h_{h_{new}}^2$$

$$- g\left(\frac{1}{6}\rho_0 \alpha \frac{N^2}{g\alpha} d^3 + \frac{1}{2}\rho_2 d + \rho_1 h_1 d + \frac{1}{2}\rho_1 h_1^2\right) \tag{16}$$

and the corresponding rate of GPE increase is

$$q_{GPE} = \frac{1}{T_{life}} \iint_A \Delta\chi \, dx \, dy, \tag{17}$$

where T_{life} is the lifetime of the tropical cyclone.

The initial conditions of the model at any given location along the track of the tropical cyclone, including h_1, T_1, T_2, and N^2, were specified from Levitus98 monthly mean climatology data. The new temperature,

T_{new}, was chosen as the minimum temperature, calculated from the model, at a given location during the whole process of the passing through of a tropical cyclone. The thickness of the mixed layer after stirring h_{new} and thus the thickness d before stirring were obtained from the conservation of mass and heat content.

3. The oceanic response to a moving tropical cyclone

As an example, the oceanic response to a tropical cyclone moving from right to left with a speed 7.5 m s^{-1} is shown in Fig. 4. The center of tropical cyclone is located at a distance of 250 km to the left edge of this map. The colors indicate the thickness of the oceanic mixed layer, and the black arrows show the direction and speed of the surface currents. The mixed layer deepens greatly, particularly to the right of the track and trailing the center of the tropical cyclone. The strongest currents are located to the right of the tropical cyclone track, which is directly related to the strong wind on the right side of the tropical cyclone.

The pattern of the ocean currents responding to the tropical cyclone in Fig. 4 is similar to the Kármán vortex street well known in classical fluid mechanics. For an observer standing in a coordinate system moving with the center of the tropical cyclone, the tropical cyclone can be thought of as a cylinder fixed in these coordinates, and water flows toward the "cylinder" from left to right. When the speed of water reaches a critical value, the Kármán vortex street would appear.

There are major differences between the traditional Kármán vortices and the vortexlike pattern in the upper ocean associated with the passing of a tropical cy-

clone. In the left far field, the anticlockwise wind stress can drive the water at first moving in the direction of the wind. As time progresses, the Coriolis force turns the ocean currents to the right. The direction of wind and current at any point left and right to the track of a tropical cyclone in the Northern Hemisphere was discussed by Emanuel (2005). If the wind stress lasted for only a short time, we would observe a current that first moves in the same direction as the wind but gradually turned to the right. Given enough time, the current would go all the way around the compass until it was headed in the same direction as it started. However, if the wind stress lasted forever, that is, the translation speed of the tropical cyclone were zero, the current would be in the same direction as the wind, that is, a circular velocity field. However, if the Coriolis force were not taken into account in the ocean model, the current pattern in Fig. 4 would not appear and the current would move around the compass as an ellipse. For a realistic case, the rotation of the current vector at a given station can be identified from Fig. 4. Since the translation velocity (7.5 m s^{-1}) is much larger than the current speed (on the order of 1 m s^{-1} or less), the time evolution of current at a given station can be viewed from a section with a constant distance from the x axis, say $y = 50$ km north of the track. The current along this section gradually rotates clockwise in the downstream direction, as explained above.

Tropical cyclones produce anomalous cold wakes. The main cause of the sea surface cooling is due to mixing of cold water from subsurface layer to the surface. The coldest water appears where the mixed layer is deepest, that is, bias to the right of the track. Price (1981) showed that the rightward bias of the temperature anomalies results from the near resonance of the storm's wind field with inertial oscillations to the right of the track, where the wind veers around the compass. Figure 5 shows the time evolution of the sea surface temperature of a station on the right side of the tropical cyclone track in the numerical experiment. There is a sudden drop of sea surface temperature, taking place during the arriving of the tropical cyclone. However, the air–sea heat exchange is not included in the ocean model, so in the experiment the relaxation of the sea surface temperature back to the initial condition takes a much longer time. In fact, even at the time when the station is out of the computational domain in the model, sea surface temperature has not fully recovered. On the other hand, the GPE calculation is based on the first half of the sea surface temperature cycle, so the detail of temperature recovery does not affect the calculation of GPE increase induced by tropical cyclone.
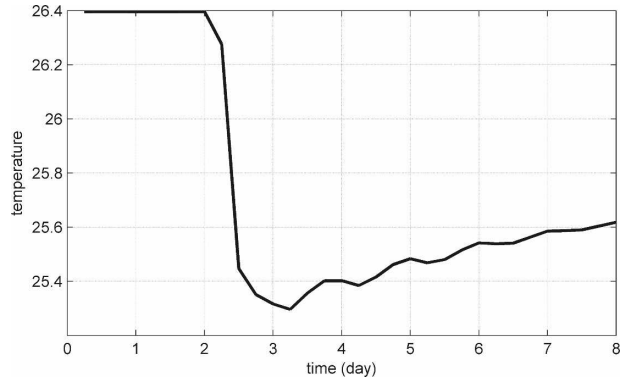

FIG. 5. The time series of the sea surface temperature at a station on the right-hand side of the hurricane track.

4. Spatial/temporal distribution of energy input induced by a tropical cyclone

A tropical cyclone works as a very efficient thermal engine converting the thermal energy released from the ocean to the atmosphere in forms of latent heat, into mechanical energy. On the other hand, motions in ocean induced by the tropical cyclone are primarily driven by the wind stress, not by the thermal energy in the ocean. In fact, all motions in the ocean related to the tropical cyclone are sustained by energy from wind stress. Most part of the mechanical energy received by the ocean is dissipated locally in the upper ocean through turbulence and waves. The remaining energy is left behind the tropical cyclone in forms of organized large-scale motions in the wake.

The energy input to the ocean induced by a tropical cyclone can be calculated using the hurricane–ocean coupled model and the formula discussed above. The mean rate of energy flux and the GPE increase for an individual tropical cyclone during its lifetime are calculated as follows:

$$\overline{q}_{\text{wave}} = \frac{1}{T_{\text{life},i}} \int_{T_{0,i}}^{T_{\text{life},i}} q_{\text{wave}} \, dt, \qquad (18)$$

$$\overline{q}_{\text{current}} = \frac{1}{T_{\text{life},i}} \int_{T_{0,i}}^{T_{\text{life},i}} q_{\text{current}} \, dt, \qquad (19)$$

$$\overline{q}_{ni} = \frac{1}{T_{\text{life},i}} \int_{T_{0,i}}^{T_{\text{life},i}} q_{ni} \, dt, \qquad (20)$$

$$\overline{q}_{\text{GPE}} = \frac{1}{T_{\text{life},i}} \int_{T_{0,i}}^{T_{\text{life},i}} q_{\text{GPE}} \, dt, \qquad (21)$$

where $T_{0,i}$ and $T_{\text{life},i}$ are the beginning and lifetime of the ith tropical cyclone in a year.

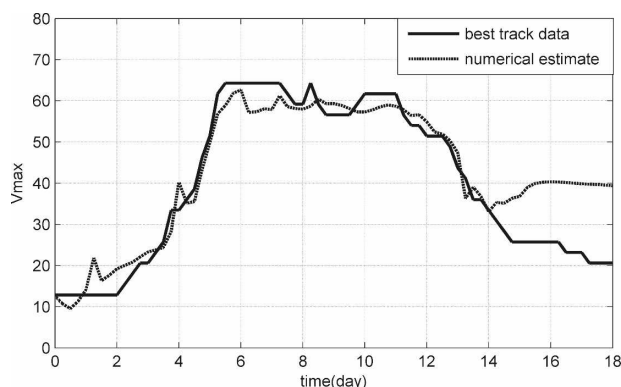As an example, we examine the energetics of Hurri-

FIG. 6. Maximum wind speed (m s^{-1}) of Hurricane Edouard estimated from the "best track" data (solid line) and from the model (dashed line).
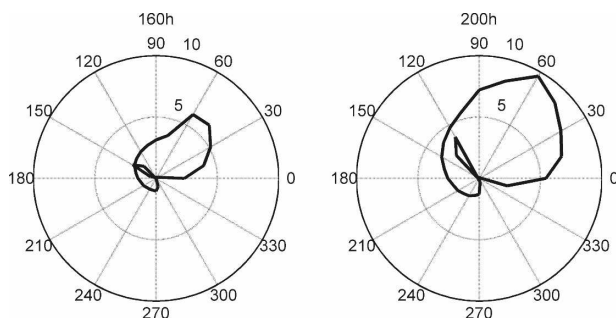

FIG. 7. Azimuthal distribution of the instantaneous energy input to surface currents at 160 and 200 h. The hurricane moved westward. The energy was calculated using $w(\theta) = \int_0^\infty (\tau \mathbf{u}) r \, dr$ (units: GW rad^{-1}).

cane Edouard, which occurred in the North Atlantic from August to September 1996. The evolution of the maximum wind speed of Edouard is shown in Fig. 6. This hurricane achieved hurricane strength, topping out at approximately 64 m s^{-1} on the fifth day. The last part of the simulation of the storm intensity is relatively poor because there is no vertical wind shear term in the three-dimensional coupled model. Our model simulation produced a wake with a temperature anomaly of $-3.1°$C averaged over an area of 400 km in the cross-track direction and 2000 km in the along-track direction, which is very close to the averaged $-3°$C cooling derived from satellite data (Emanuel 2001).

Using Eqs. (18)–(21), the energy input to surface waves by Hurricane Edouard is estimated as 7.3 TW. This is a huge energy input released over a very short time period (18 days). The energy input to surface currents is 0.40 TW, including 0.12 TW for the energy input to the Ekman layer over the near-inertial frequency, and the increase of GPE is estimated as 0.16 TW.

The spatial distribution of the instantaneous energy input to surface currents at 160 and 200 h is shown in Fig. 7. The center of the hurricane is located at the origin of the polar coordinates and moves westward. The energy input is highly asymmetric with respect to the hurricane center. In fact, 45° to the right side behind the hurricane, surface currents flow in the same direction as the wind (Fig. 4). Thus, the regime of maximal rate of energy input occurs to the right side behind the hurricane center. On the other hand, energy input to the left side behind the hurricane center is small. In particular, it is negative at 30° to the left-hand side of the hurricane track, indicating that local current flows in the direction opposite to the local wind.

On the other hand, the energy input to surface waves is distributed in the form of an irregular circle, corre-

sponding to the pattern of wind stress amplitude, but it is independent of wind stress direction. Figure 8 shows the time evolution of the instantaneous energy input to surface waves at three stations fixed in the Eulerian coordinates. Note that energy input to the station on the right side of the hurricane is the largest. The double peak structure of the energy input to the station located on the track of the hurricane center is due to the existence of the eyewall, where the wind stress was very small. The station to the left side of the hurricane receives the smallest amount of energy from the wind.

The time evolution of the instantaneous energy input to surface currents induced by Hurricane Edouard is shown in Fig. 9. Note that the variation of the total energy generated is associated with the episodic changes in the intensity and the structure (such as the radius of the maximum wind) of the storm.
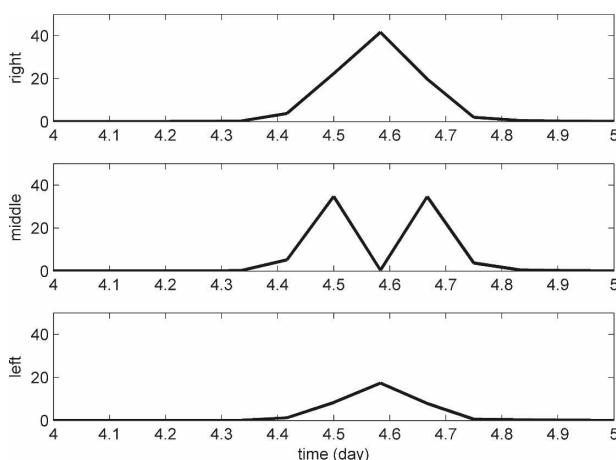

FIG. 8. Temporal evolution of the instantaneous energy input (W m^{-2}) to surface waves at three fixed stations: (top) a station on the right-hand side of the hurricane track, (middle) a station on the hurricane track, and (bottom) a station on the left-hand side of the hurricane track.
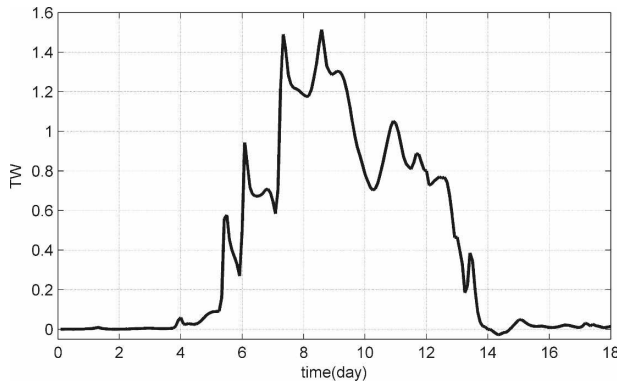
FIG. 9. Temporal evolution of the instantaneous energy input to surface currents induced by Hurricane Edouard.

Despite many differences between patterns of wind and the corresponding energy input to the ocean, they share the most outstanding common feature that reflects the asymmetric nature with respect to the storm track.

5. Global contribution due to the tropical cyclones

Tropical cyclones vary greatly in their location and strength; thus, energy generated from an individual storm may not be representative for their contribution to the climate system. Each year, there are many tropical cyclones in the world's oceans; thus, the most objective approach is to estimate the annual mean contribution from these storms. We calculated the energy input to the ocean induced by over 1500 tropical cyclones from 1984 to 2003, based on the hurricane–ocean coupled model discussed above. The annual mean energy input is defined as

$$Q_{\text{wave}} = \left(\sum_{i=1}^{N} \overline{q}_{\text{wave},i} \, T_{\text{life},i} \right) \bigg/ T_{\text{year}}, \qquad (22)$$

$$Q_{\text{current}} = \left(\sum_{i=1}^{N} \overline{q}_{\text{current},i} \, T_{\text{life},i} \right) \bigg/ T_{\text{year}}, \qquad (23)$$

$$Q_{ni} = \left(\sum_{i=1}^{N} \overline{q}_{ni,i} \, T_{\text{life}} \right) \bigg/ T_{\text{year}}, \qquad (24)$$

$$Q_{\text{GPE}} = \left(\sum_{i=1}^{N} \overline{q}_{\text{GPE},i} \, T_{\text{life},i} \right) \bigg/ T_{\text{year}}, \qquad (25)$$

where N is the total number of tropical cyclones of a specific year, $\overline{q}_{\text{name},i}$ is the mean rate of energy input from the ith tropical cyclone for each kind of energy input, and T_{year} the time of a year.

The best-track data were downloaded from the K. A. Emanuel Web site (cited above). Tropical cyclones

with a maximal recorded wind speed less than 17 m s^{-1} were not included in the following discussions. Based on Eqs. (22)–(25) the annual mean energy input over the past 20 years can be estimated. Wind energy input to surface waves induced by tropical cyclones is 1.62 TW; the energy input to surface currents is estimated as 0.10 TW, including 0.03 TW for the energy input to the near-inertial motions; and the increase of GPE is 0.05 TW.

Nilsson (1995) made an attempt at estimating the global power input to the near-inertial waves due to hurricanes, where he gave an estimate as 0.026 TW, comparable with the results obtained in this study. However, using the average downward vertical energy flux of $2 \text{ ergs cm}^{-2} \text{ s}^{-1}$ based on the observed velocity profile during the passage of Hurricane Gilbert, Shay and Jacob (2006) gave an estimation of the near inertial energy flux as 0.74 TW, which is much larger than our estimate.

The relationship between the increase of GPE and the energy input to the near-inertial currents and the surface currents for each individual tropical cyclone over the past 20 years are demonstrated in Figs. 10a and 10b, respectively. It is clearly seen that the near-inertial energy input alone cannot account for the increase of the GPE when the hurricanes are strong. The ratio of GPE increase to the wind energy input to the near-inertial currents and the total surface currents versus normalized PDI (power dissipation index: $\text{PDI} \equiv \int_{0}^{T_{\text{life}}} v_{\text{max}}^{3} \, dt$, which indicates the strength of the tropical cyclone) are shown in Figs. 10c and 10d, respectively. For weak topical cyclones the increase of GPE is limited and it may be dominated by the contribution from the near-inertial energy from the wind. For hurricanes, however, the near-inertial energy from the wind can only supply a small portion of the energy needed for GPE increase, and the remaining portion of energy should be supplied by subinertial components of the wind energy input to the surface currents. Therefore, when the hurricane is strong, wind energy input to the subinertial motion is not totally dissipated in the mixed layer; instead, it contributes to the increase of GPE. Moreover, the conversion rate of kinetic energy input from the wind to GPE also increases as the strength of the hurricane increases.

The distribution of the energy input to the near-inertial motions from tropical cyclones averaged from 1984 to 2003 is shown in Fig. 11. Although this energy is only 5% of that from smoothed wind field, most of this energy is distributed in the latitudinal band from 10° to 30°N in the western Pacific and in the North Atlantic, with approximately half of the total energy being input into the western North Pacific. For ex-
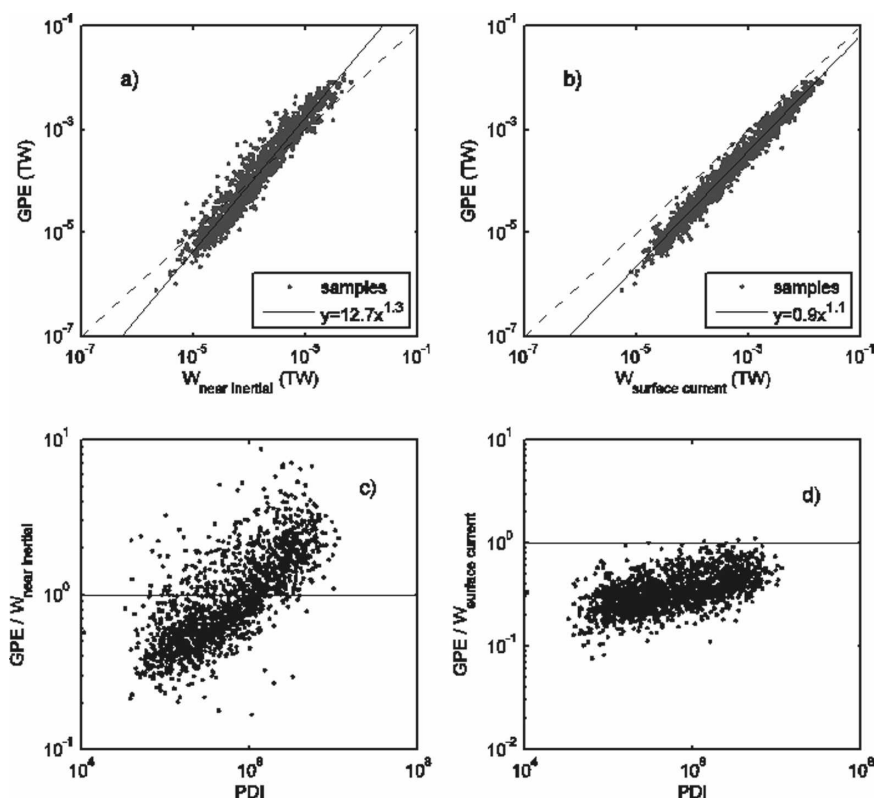
FIG. 10. Relationship between the increase of GPE and the energy sources from the hurricanes: (a) GPE vs near-inertial components, (b) GPE vs wind energy input to the surface currents, (c) the ratio of GPE increase to near-inertial energy from the wind vs PDI, and (d) the ratio of GPE increase to energy from the wind input to the surface current vs PDI. In the upper panels the solid lines indicate best-fit power laws.

ample, at 20°N the ratio of the zonal average of near-inertial energy generated by tropical cyclones and that calculated from the smoothed wind stress data (Alford 2003) is approximately 0.6:1. (The distribution of the other forms of energy generated from tropical cyclones has similar patterns.)

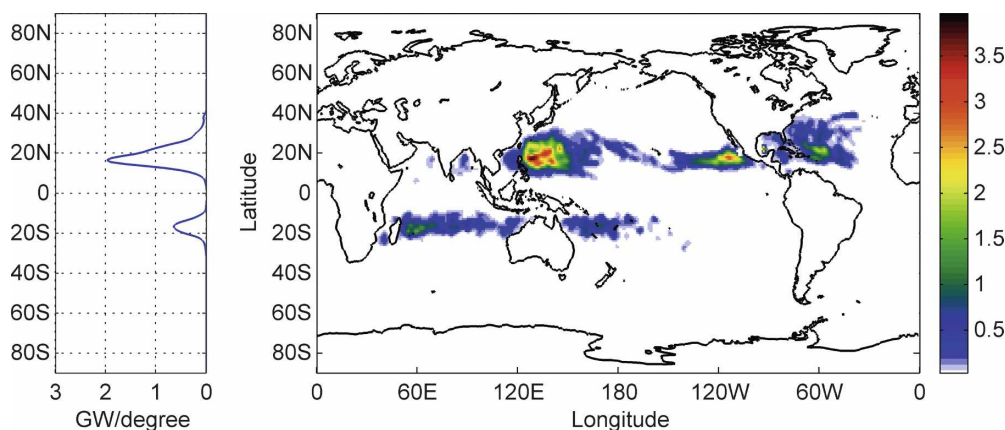Figure 12 shows the distribution of the energy input to surface waves (induced by smoothed NCEP–NCAR

FIG. 11. (right) Energy input to near-inertial motions induced by tropical cyclones averaged from 1984 to 2003 (units: mW m^{-2}); (left) the meridional distribution of the integrated energy.
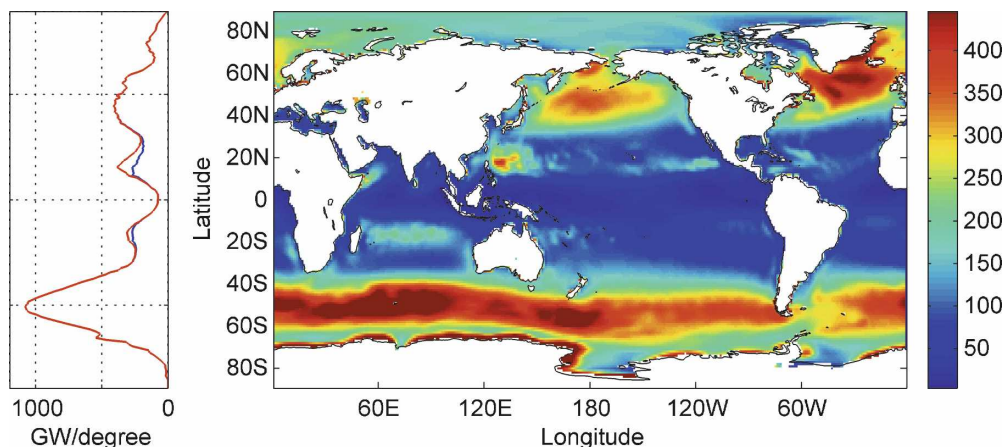
FIG. 12. (right) Distribution of energy input generated from smoothed wind field and tropical cyclones to surface waves averaged from 1984 to 2003 (units: mW m^{-2}) and (left) the meridional distribution of the zonal integrated energy source. The blue line is the energy input generated by smoothed wind stress, and the red line is the total energy input, including contributions due to tropical cyclones.

wind field and tropical cyclones) averaged from 1984 to 2003. The left panel is the meridional distribution of the zonally integrated results, where the blue line is the energy input from the smoothed wind field and the red line is the total energy input. From the meridional distribution, it is readily seen that the energy generated by tropical cyclones greatly enhances the energy input at the midlatitude. In the latitudinal band from 10° to 30°N, tropical cyclones account for 22% increase of the energy, and in the northwest Pacific, they account for 57% increase of energy, compared with results calculated from smoothed wind data. Although the total amount of energy input by tropical cyclones is much smaller than that by smoothed wind field, it may be more important for many applications including ecology, fishery, and environmental studies since they occur at the midlatitude band where the stratification is strong during a short time period.

Figure 13 shows the decadal variability of the normalized annual mean energy input to the ocean (including surface waves and surface currents) induced by tropical cyclones, the energy input to the ocean based on the NCEP–NCAR wind stress dataset (Huang et al. 2006), and the normalized PDI. The energy input from tropical cyclones show strong interannual and decadal variability with an increasing rate of 16% over the past 20 years. By comparing PDI between the model simulations and observations, the estimate in current study is within a mean error of 18%. The increase of GPE induced by hurricanes shows a similar decadal variability during the same time period (not shown in this figure).

The tropical cyclone–induced mixing and upwelling are important factors regulating the ocean circulation

and water mass balance. The mixed layer deepening for an individual tropical cyclone is defined as the difference between the initial mixed layer depth and the maximal mixed layer depth obtained from the model at a given location during the whole process of the passing through of a tropical cyclone. However, there is a possibility that several tropical cyclones passed through the same grid point within one year; each time the mixed layer deepening is denoted as dh_j. If there are N tropical cyclones that passed through this grid in one year, the total mixed layer deepening at this grid is $dH = \Sigma_{j=1}^{N} dh_j$, and the distribution in the world's oceans is shown in Fig. 14a. The maximal mixed layer deepening induced by tropical cyclones is on the order of 100 m. The mixed layer deepening gives rise to the annual (accumulated) mean upwelling rate $w = dH/T_{\text{year}}$ (Fig. 14b). The total upwelling volume flux induced in the
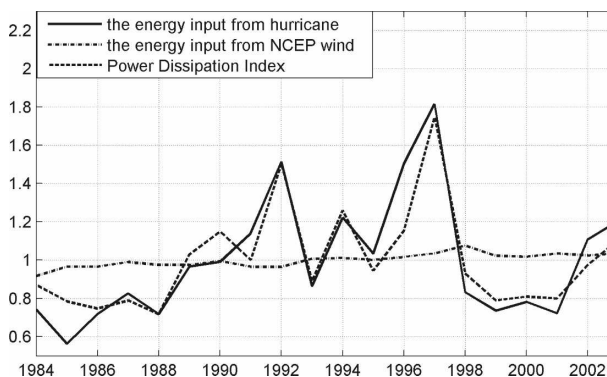

FIG. 13. The normalized annual-mean energy input to surface waves from hurricane (solid line), from the NCEP–NCAR wind stress dataset (dash–dot line) and the normalized PDI (dashed line).
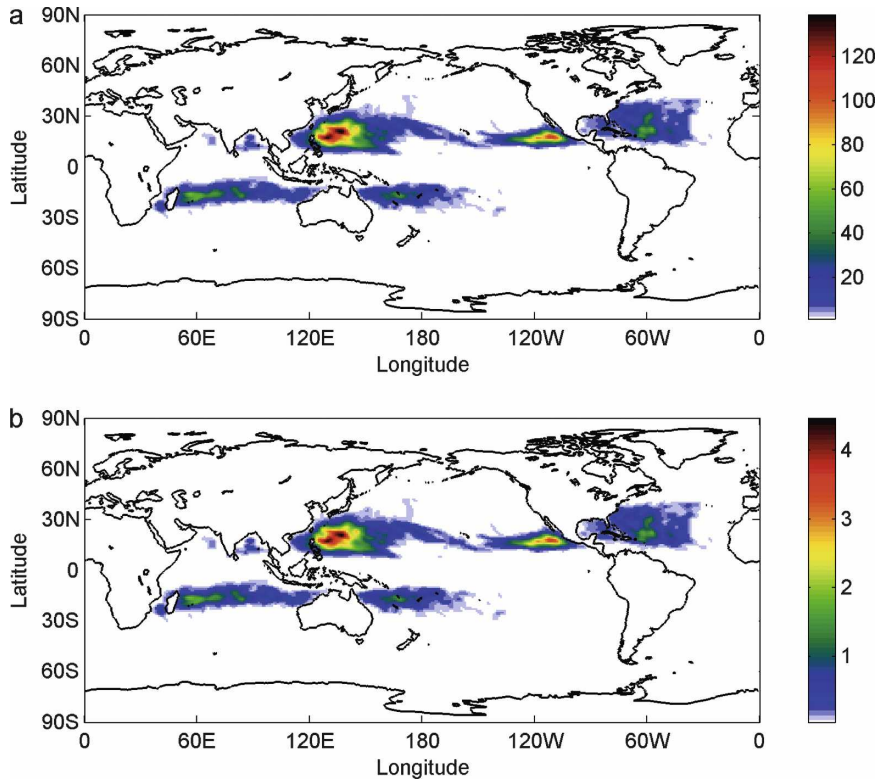
FIG. 14. (a) Annual-mean (accumulated) mixed layer deepening (m) induced by tropical cyclones averaged from 1984 to 2003 and (b) the corresponding annual mean (accumulated) upwelling velocity (units: 10^{-6} m s^{-1}).

world's oceans is estimated as 39 Sv (Sv = 10^6 m^3 s^{-1}), with 22.4 Sv in the North Pacific. Qiu and Huang (1995) discussed subduction and obduction in the oceans; they estimated that the basin-integrated subduction rate is 35.2 Sv and obduction rate is 7.8 Sv in the North Pacific ($10°$ off the equator). Therefore, the total rate of upwelling induced by tropical cyclones is approximately 50% of the subtropical water mass formation rate through subduction and it is much larger than obduction.

Consequently, tropical cyclones must have a major impact on mixing and water mass balance in the regional and global oceans. The cyclone-induced upwelling may play a role of capital importance in water mass balance in the world's oceans, and water mass balance without taking into consideration of the contribution due to cyclone-induced mixing may not be acceptable.

The vertical diffusivity averaged over the lifetime of a tropical cyclone can be defined by the following scaling: $k = w\,dh$, where dh is mixed layer deepening due to cyclone stirring, and $w = dh/T_{\text{life}}$ is the equivalent upwelling velocity averaged over the life cycle of a tropical cyclone.

However, for the study of oceanic general circulation, it is more appropriate to define the contribution due to each tropical cyclone in terms of the annual mean vertical diffusivity

$$k_j = w_j dh_j = dh_j^2/T_{\text{year}}. \tag{26}$$

The annual meaning (accumulated) vertical diffusivity is defined as

$$k = \sum_{j=1}^{N} k_j = \frac{1}{T_{\text{year}}} \sum_{j=1}^{N} dh_j^2. \tag{27}$$

The horizontal distribution of the tropical cyclone–induced vertical diffusivity (Fig. 15), is similar to the recent result of Sriver and Huber (2007). However, the results that we obtained are generally higher. Sriver and Huber assumed that all mixing in a given year is achieved during the single largest event; we have assumed that mixing due to each hurricane that passed through the same grid in one year all contribute to mixing. Our results indicate that vertical diffusivity induced by tropical cyclones is on the order of $(1 - 6) \times 10^{-4}$ m^2 s^{-1}, which is approximately 10 to 100 times larger than the low environmental diffusivity
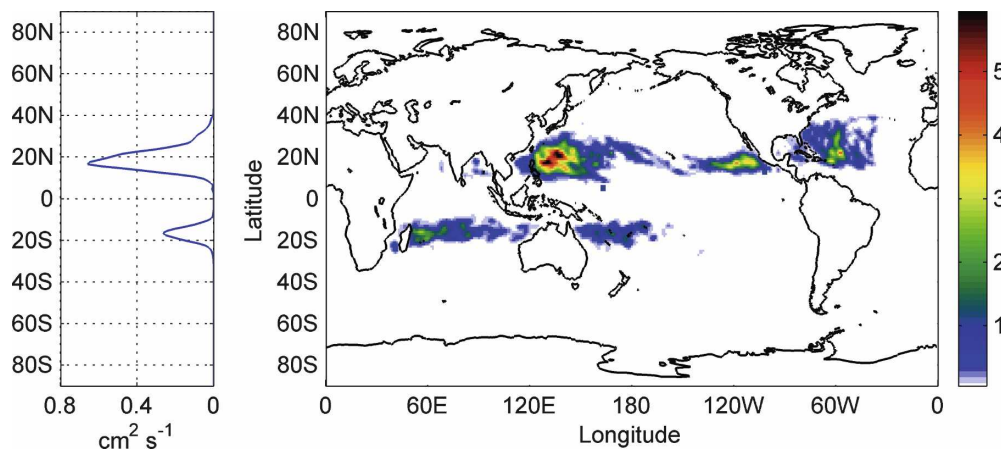
FIG. 15. Annual-mean vertical diffusivity induced by tropical cyclones from 1984 to 2003 (units: 10^{-4} $m^2\,s^{-1}$): (right) the horizontal distribution and (left) the zonally averaged vertical diffusivity.

$(0.05 - 0.1) \times 10^{-4}\ m^2\ s^{-1}$ observed in the subtropical ocean below the mixed layer. Although the hurricane-induced mixing takes place in a vertical location in the water column quite different from that of deep mixing induced by tides, they all contribute to the maintenance of the oceanic general circulation. Previous studies showed that mixing at low latitude can enhance the meridional overturning circulation and poleward heat flux (Scott and Marotzke 2002; Bugnion et al. 2006; Huang et al. 2007). Thus, tropical cyclones, especially strong hurricanes, can play an important role in driving the global thermocline circulation.

6. Conclusions

Mechanical energy input to the ocean induced by 1500 tropical cyclones during 1984 to 2003 were estimated based on a hurricane–ocean coupled model. The annual mean energy input to surface waves induced by tropical cyclones is estimated as 1.62 TW and the energy input to surface currents is estimated as 0.10 TW (including 0.03 TW to the near-inertial motions). The annual mean increase of GPE is estimated as 0.05 TW. Both the energy input from tropical cyclones and the increase of GPE of the ocean show strong interannual and decadal variability with an increase of 16% within the past 20 years.

Tropical cyclones also affect the water mass balance in the world's oceans. The annual mean diapycnal upwelling induced by tropical cyclones over the past 20 years is estimated as 39 Sv. Diapycnal diffusivity in the ocean is greatly enhanced due to tropical cyclones. Within the regimes of strong activity of tropical cyclones, the increase of diapycnal diffusivity is on the order of $(1 - 6) \times 10^{-4}\ m^2\ s^{-1}$.

Our study is only the first step toward unraveling the complicated roles of hurricanes in the global energetics. There are several shortcomings in the formulation of the coupled model. First of all, wind energy input to the surface waves is not included in the current model. It is speculated that a model including wind energy input to surface waves may greatly enhance the production of GPE increase due to the stirring by subtropical cyclones. The monthly mean Levitus data cannot describe the oceanic conditions under tropical cyclones accurately. The absence of the air–sea heat flux in the model may underestimate the sea surface cooling. The entrainment parameterization cannot account for all the turbulence resources. Finally, the difference in the structure of individual tropical cyclones, such as the radius of the maximal wind velocity and the assumption of axisymmetry, between the model simulation and the observations may induce further discrepancy.

In addition, the connection between tropical cyclone–induced mixing and the meridional overturning circulation remains unclear at the present time. For example, tropical cyclones are active only for a small portion of the annual cycle. A natural question is then, How does the energy input induced by tropical cyclones at the low and midlatitudes over a small fraction of time in a year affect the general oceanic circulation? To answer these questions further study is clearly needed, and we hope this study will stimulate interest in exploring the contribution of hurricanes in the global climate machinery.

REFERENCES

Alford, M. H., 2003: Improved global maps and 54-year history of wind-work done on the ocean inertial motions. *Geophys. Res. Lett.,* **30,** 1424, doi:10.1029/2002GL016614.

Bugnion, V., C. Hill, and P. H. Stone, 2006: An adjoint analysis of the meridional overturning circulation in an ocean model. *J. Climate,* **19,** 3732–3750.

Cooper, C., and J. D. Thompson, 1989: Hurricane-generated currents on the outer continental shelf. Part I: Model formulation and verification. *J. Geophys. Res.,* **94,** 12 513–12 539.

D'Asaro, E. A., 1985: The energy flux from the wind to near-inertial motions in the mixed layer. *J. Phys. Oceanogr.,* **15,** 943–959.

Emanuel, K. A., 1988: Toward a general theory of hurricanes. *Amer. Sci.,* **76,** 370–379.

——, 1989: The finite amplitude nature of tropical cyclogenesis. *J. Atmos. Sci.,* **46,** 3431–3456.

——, 2001: The contribution of tropical cyclones to the oceans' meridional heat transport. *J. Geophys. Res.,* **106** (D14), 14 771–14 781.

——, 2005: Increasing destructiveness of tropical cyclones over the past 30 years. *Nature,* **436,** 686–688, doi:10.1038/nature03906.

Garrett, J. R., 1977: Review of drag coefficients over oceans and continents. *Mon. Wea. Rev.,* **105,** 915–929.

Huang, R. X., W. Wang, and L. L. Liu, 2006: Decadal variability of wind-energy input to the world ocean. *Deep-Sea Res. II,* **53,** 31–41.

——, C. J. Huang, and W. Wang, 2007: Dynamical roles of mixed layer in regulating the meridional mass/heat fluxes. *J. Geophys. Res.,* **112,** C05036, doi:10.1029/2006JC004046.

Munk, W., and C. Wunsch, 1998: Abyssal recipes II. Energetics of tidal and wind mixing. *Deep-Sea Res. I,* **45,** 1977–2010.

Nilsson, J., 1995: Energy flux from traveling hurricanes to the internal wave field. *J. Phys. Oceanogr.,* **25,** 558–573.

Plueddemann, A. J., and J. T. Farrar, 2006: Observations and models of the energy flux from the wind to mixed-layer inertial currents. *Deep-Sea Res. II,* **53,** 5–30.

Pollard, R. T., and R. C. Millard, 1970: Comparison between observed and simulated wind-generated inertial oscillations. *Deep-Sea Res.,* **17,** 153–175.

Price, J. F., 1981: Upper ocean response to a hurricane. *J. Phys. Oceanogr.,* **11,** 153–175.

——, 1983: Internal wave wake of a moving storm. Part I: Scales, energy budget and observations. *J. Phys. Oceanogr.,* **13,** 949–965.

——, R. A. Weller, and R. Pinkel, 1986: Diurnal cycling: Observations and models of the upper ocean response to diurnal hearing, cooling, and wind mixing. *J. Geophys. Res.,* **91** (C7), 18 411–18 427.

Qiu, B., and R. X. Huang, 1995: Ventilation of the North Atlantic and North Pacific: Subduction versus obduction. *J. Phys. Oceanogr.,* **25,** 2374–2390.

Schade, L. R., and K. A. Emanuel, 1999: The ocean's effect on the intensity of tropical cyclones: Results form a simple Coupled Atmosphere–Ocean Model. *J. Atmos. Sci.,* **56,** 642–651.

Scott, J. R., and J. Marotzke, 2002: The location of diapycnal mixing and the meridional overturning circulation. *J. Phys. Oceanogr.,* **32,** 3578–3595.

Shay, L. K., and S. D. Jacob, 2006: Relationship between oceanic energy fluxes and surface winds during tropical cyclone passage. *Atmosphere-Ocean Interactions II: Advances in Fluid Mechanics,* W. Perrie, Ed., WIT Press, Southampton, United Kingdom, 115–142.

Sriver, R. L., and M. Huber, 2007: Observational evidence for an ocean heat pump induced by tropical cyclones. *Nature,* **447,** 577–580, doi:10.1038/nature05785.

Wang, W., and R. X. Huang, 2004a: Wind energy input to the surface waves. *J. Phys. Oceanogr.,* **34,** 1276–1280.

——, and ——, 2004b: Wind energy input to the Ekman layer. *J. Phys. Oceanogr.,* **34,** 1267–1275.

Watanabe, M., and T. Hibiya, 2002: Global estimate of the wind-induced energy flux to the inertial motion in the surface mixed layer. *Geophys. Res. Lett.,* **29,** 1239, doi:10.1029/2001GL04422.

Wunsch, C., 1998: The work done by the wind on the oceanic general circulation. *J. Phys. Oceanogr.,* **28,** 2332–2340.